JOURNAL OF SOLID STATE CHEMISTRY **14**, 99–111 (1975).

Ultramicrostructural Characteristics of Some Intercalates of Graphite: An Electron Microscopic Study

E. L. EVANS AND J. M. THOMAS

Edward Davies Chemical Laboratories, The University College of Wales, Aberystwyth, SY23 1NE, United Kingdom

Received July 8, 1974

The ultramicrostructure of certain graphite–intercalate residue compounds known to exhibit ordering has been investigated using high-resolution transmission electron microscopy and electron diffraction. Some novel ternary graphite–intercalates formed as a result of interactions between existing intercalates and other guest species have also been investigated. The superlattice patterns associated with the ordering of the intercalating species are readily interpretable, and it has been possible to obtain direct lattice images of the $\{10\bar{1}0\}$ graphite (0.21 nm) of the $\{100\}$ intercalated $FeCl_3$ (0.52 nm) and of $\{10\bar{1}0\}$ intercalated potassium (0.36 nm). It is shown that potassium acts as an effective reducing agent, and, in the graphite–ferric chloride–potassium system, free iron and potassium chloride are formed. The catalytic activity of this ternary intercalate is probably associated with highly dispersed free iron.

1. Introduction

A number of atomic and molecular species in various electronic states can be accommodated between the layers of materials with lamellar structures such as graphite (*1*), the transition metal dichalcogenides (*2*), and certain sheet silicates (*3*), thus causing the crystal to swell. These changes are readily detectable by X-ray diffraction methods which yield space-averaged structural information. Despite the fact that intercalates are often suitable for high-resolution electron microscopy and selected area electron diffraction techniques, comparatively little work has been carried out to elucidate the structures of these materials. For example, of the 40 or so known intercalates of graphite, electron diffraction studies have been reported for only a few: graphite–potassium (*4*), graphite–halogen (*5*, *6*), graphite–ferric chloride (*7*) and graphite–molybdenum pentachloride (*8*).

It is now generally agreed (*9*) that, upon appropriate undersaturation such as vapour pressure reduction, and even when the pressure of intercalant is ultimately zero, a certain proportion of the guest species remains between the layers, thus forming a stable residue compound. It is thought (*10*) that the intercalating species is trapped by lattice imperfections to form isolated islands. Detailed structural information on such compounds, however, is difficult to obtain by conventional single crystal X-ray diffraction techniques since the data are collected from a relatively large volume of material and thus only an averaged structure is obtained. The availability of microbeam[1] (or selected area) electron diffraction techniques and high-resolution electron microscopy, which can resolve particular lattice planes of the crystal, however, avoids some of the inherent difficulties of interpreting the X-ray patterns and permits the limit of the technique a projection of the structure of the layer planes to be inferred directly from electron-diffraction effects, provided due cognisance is taken of multiple and inelastic scattering processes.

In view of the recent interest shown in the catalytic potentialities of certain ternary

---

[1] With our instrument (Philips EM 300) areas with diameters as small as 10 μm could be analysed.

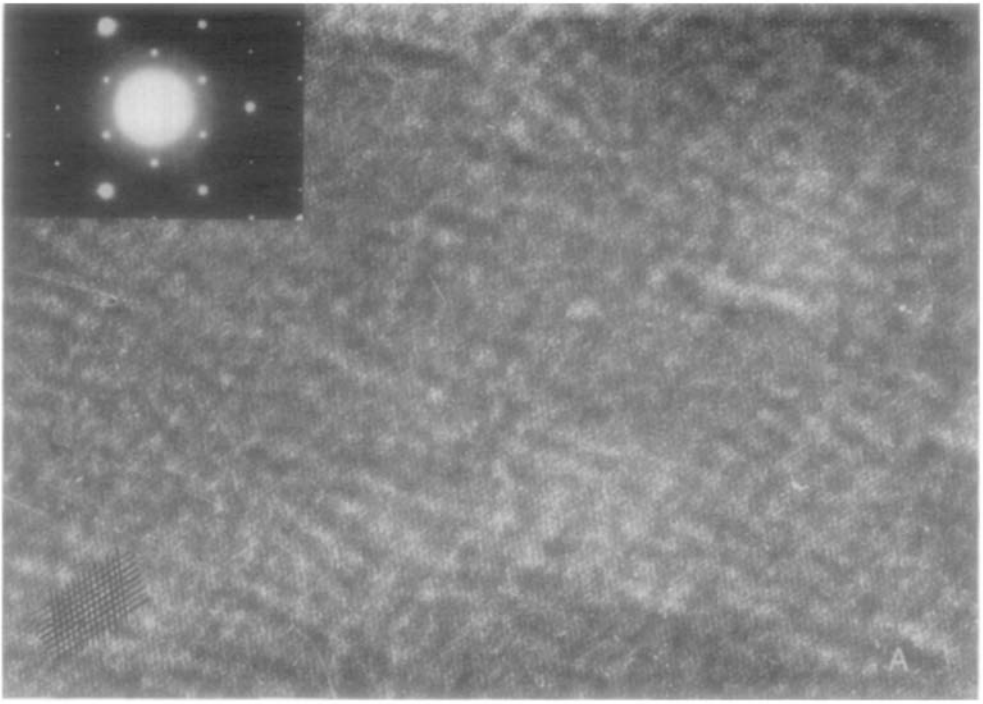

FIG. 1A. Phase-contrast high-resolution image of two of the three $\{10\bar{1}0\}$ lattices of graphite separated by 0.21 nm. The corresponding diffraction pattern is shown in the inset.

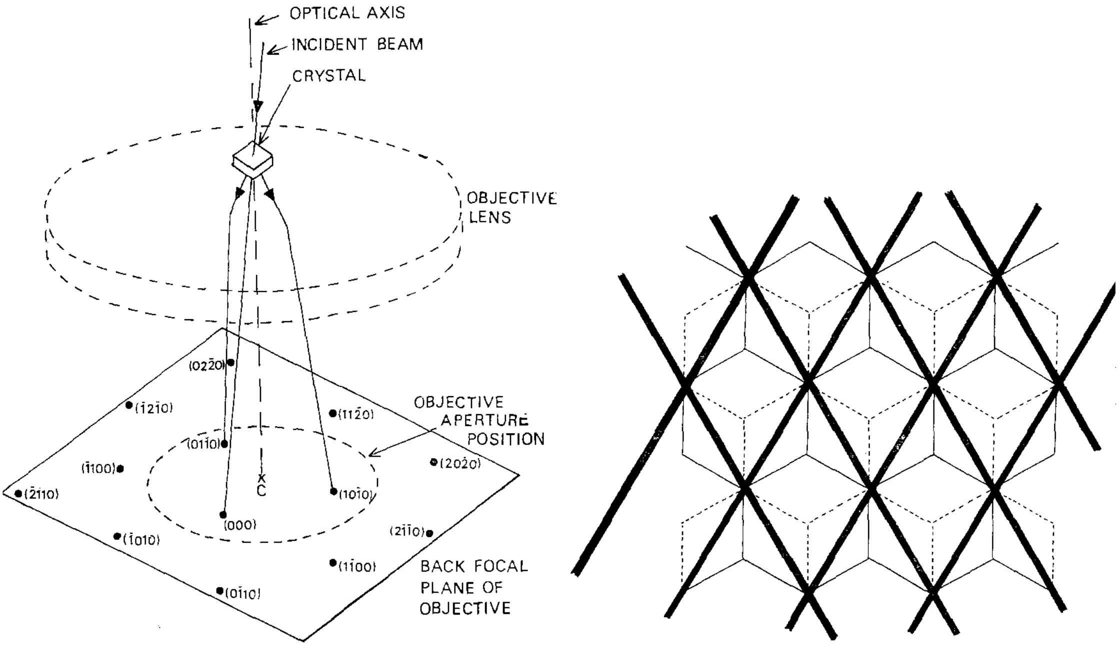

FIG. 1B. Schematic representation of the three-beam tilted illumination arrangement employed to obtain Fig. 1A. C. Schematic representation of the fringe pattern configuration shown in Fig. 1A. (The fringes delineate the unit meshes of graphite.)

graphite intercalates (*11*), such as graphite–ferric chloride–potassium, we undertook a detailed study of this material. It was felt that a better understanding of the structure of this material would be obtained by carrying out, in addition, a reexamination of the structures of graphite–potassium, graphite–ferric chloride, and graphite–bromine and to investigate the nature and structure of other possible ternary compounds such as graphite–potassium–bromine.

2. Materials

The graphite crystals employed in the investigation were naturally occurring specimens (obtained from Ticonderoga, N.Y.) which had been subjected to stringent purification procedures (*12*). Samples suitable for transmission electron microscopy (less than 100 nm thick) were obtained by repeated cleavage using adhesive tape which was subsequently dissolved in chloroform. Such cleaved single crystals invariably oriented with their basal planes parallel to the support grid, thus making it impossible to image the interlayer lattice. Such images could be obtained, however, by using powdered natural graphite (Type SP1 Union Carbide) which tends to assume a random orientation on the support grid and it was found that certain crystallites were suitably oriented to permit imaging of the interlayer lattice. The lattice images were obtained using a Philips EM 300 electron microscope.

The intercalates were prepared as follows.

(*a*) *Graphite–ferric Chloride*. Anhydrous ferric chloride and graphite were heated together in a sealed tube containing a small pressure (~0.5 Torr) of chlorine gas at 573 K for 3 days and the intercalate was freed from any excess ferric chloride by washing with dilute hydrochloric acid.

(*b*) *Graphite–bromine*. Graphite was exposed to bromine vapour in a sealed evacuated tube at room temperature for 3 days.

(*c*) *Graphite–potassium*. Graphite was exposed to potassium vapour in a sealed evacuated tube at 573 K for 24 hr.

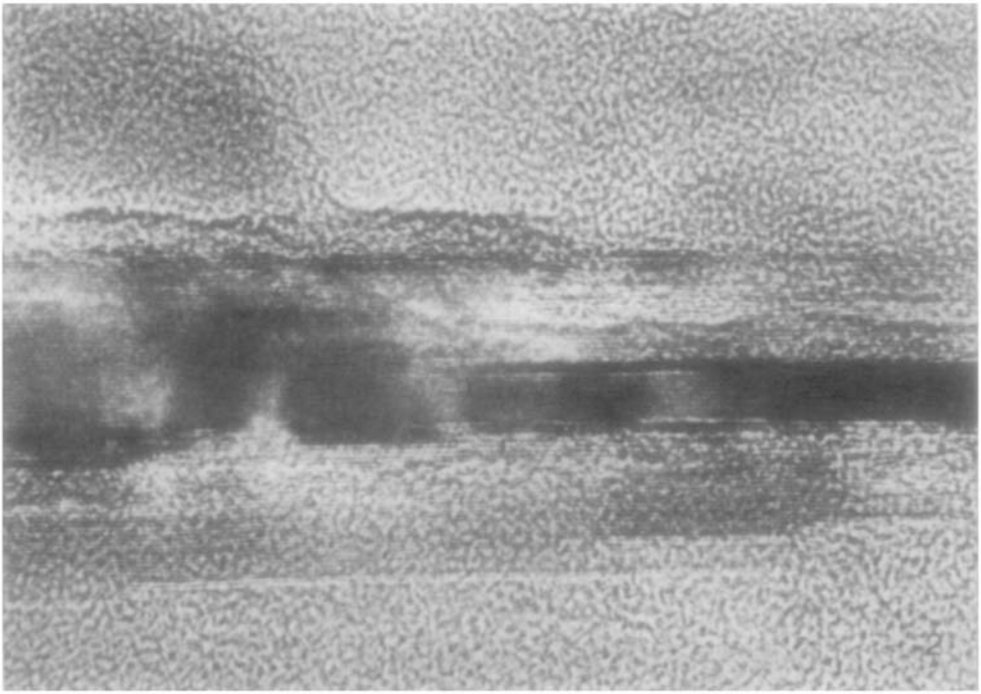

FIG. 2. Phase contrast high-resolution image of the interlayer lattice of graphite with regular spacing of 0.34 nm.

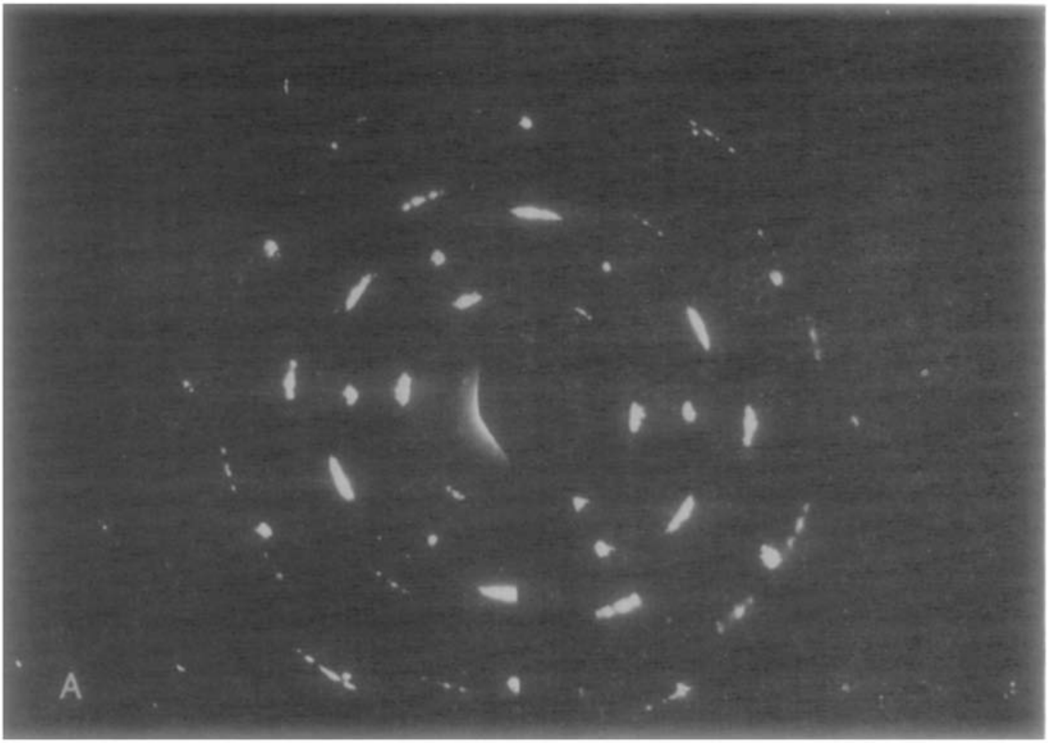

FIG. 3A. Selected area electron diffraction pattern characteristic of graphite-ferric chloride intercalate.

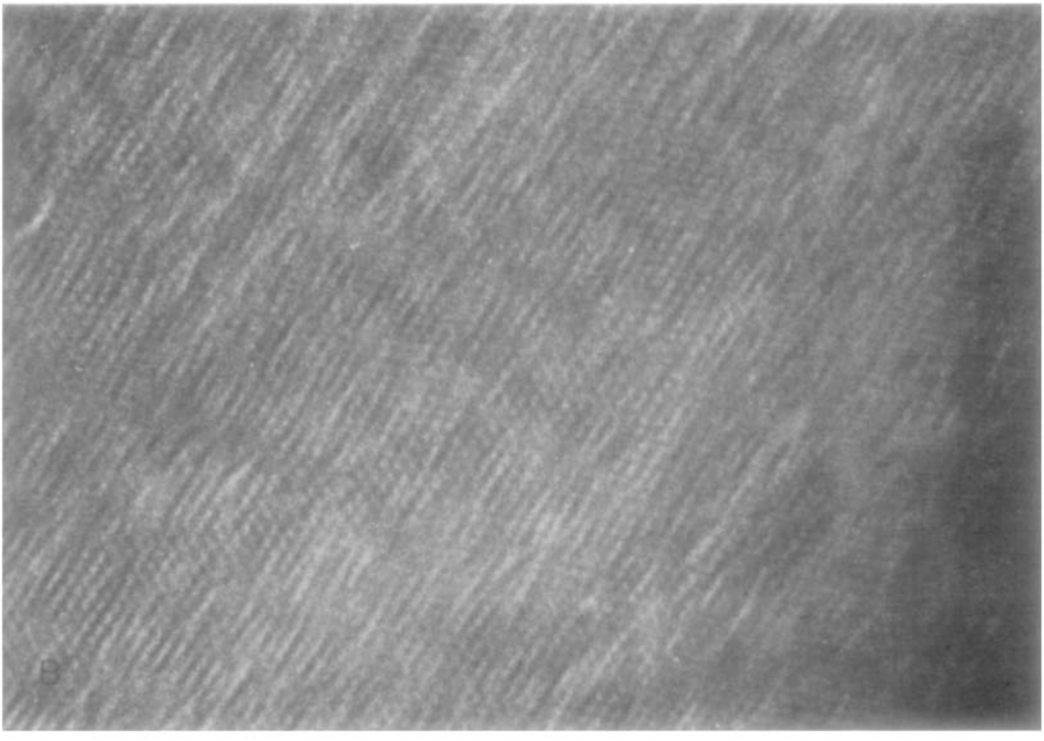

FIG. 3B. Phase contrast high resolution image of the {100} lattices of graphite-ferric chloride intercalate with spacings of 0.52 nm, using axial illumination.

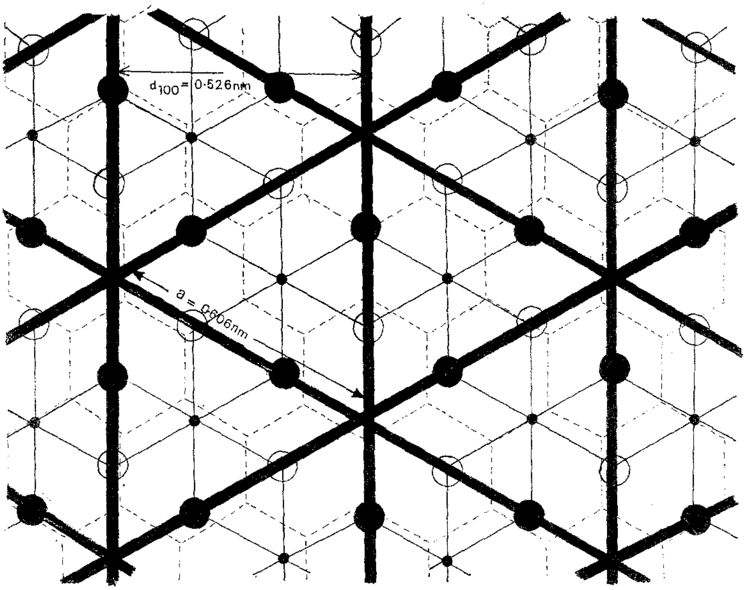

FIG. 3C. Schematic representation of a possible configuration of the image observed in Fig. 3B. The large circles represent chlorine atoms, above (open) and below (closed) the plane of iron atoms (small closed circles). The broken lines represent the graphite lattice.

(*d*) *Graphite–potassium–bromine.* Graphite–bromine was exposed to potassium vapour in a sealed evacuated tube at 573 K for 24 hr.

(*e*) *Graphite–ferric chloride–potassium.* Graphite–ferric chloride was exposed to potassium vapour in a sealed evacuated tube at 573 K for 24 hr.

3. Results and Discussion

3.1. *Unreacted Graphite*

Cleaved samples produced characteristic single crystal graphite hexagonal spot diffraction patterns. (Fig. 1A inset). We were able to obtain a phase-contrast high-resolution image of two of the three $\{10\bar{1}0\}$ planes separated by 0.21 nm (Fig. 1A). This is in excellent agreement with the accepted X-ray value of 0.213 nm. Three-beam tilted illumination was employed as shown in Fig. 1B. A possible configuration of the fringe pattern is shown schematically in Fig. 1C. (The fringes delineate the unit meshes of graphite.)

Interlayer lattice images with regular spacings of 0.34 nm are readily obtained with the powdered graphite (Fig. 2).

3.2. *Graphite–Ferric Chloride*

Graphite–ferric chloride was the first graphite intercalate to be studied by electron diffraction (7), and most of the diffraction patterns obtained in our investigation (Fig. 3A) were found to be identical to those interpreted earlier by Cowley and Ibers (7). They pointed out, and our investigation confirms their findings, that the patterns might seem at first sight to result from diffraction from a mixture of graphite and ferric chloride with the respective *a* axes of the two hexagonal lattices rotated by 30° with respect to one another around the common *c* axis. The appearance in these diffraction patterns of the forbidden $\{100\}$ ferric chloride reflections, however, suggests that there is disorder normal to the layer plane, i.e., the normal ferric chloride stacking sequence is absent resulting in an extension of $\{100\}$ reflections into finite rods in reciprocal space and their consequent appearance in the diffraction pattern. Lattice images can be obtained from these $\{100\}$ reflections (using axial illumination) and the first such image of an intercalate is shown in Fig. 3B with the requisite

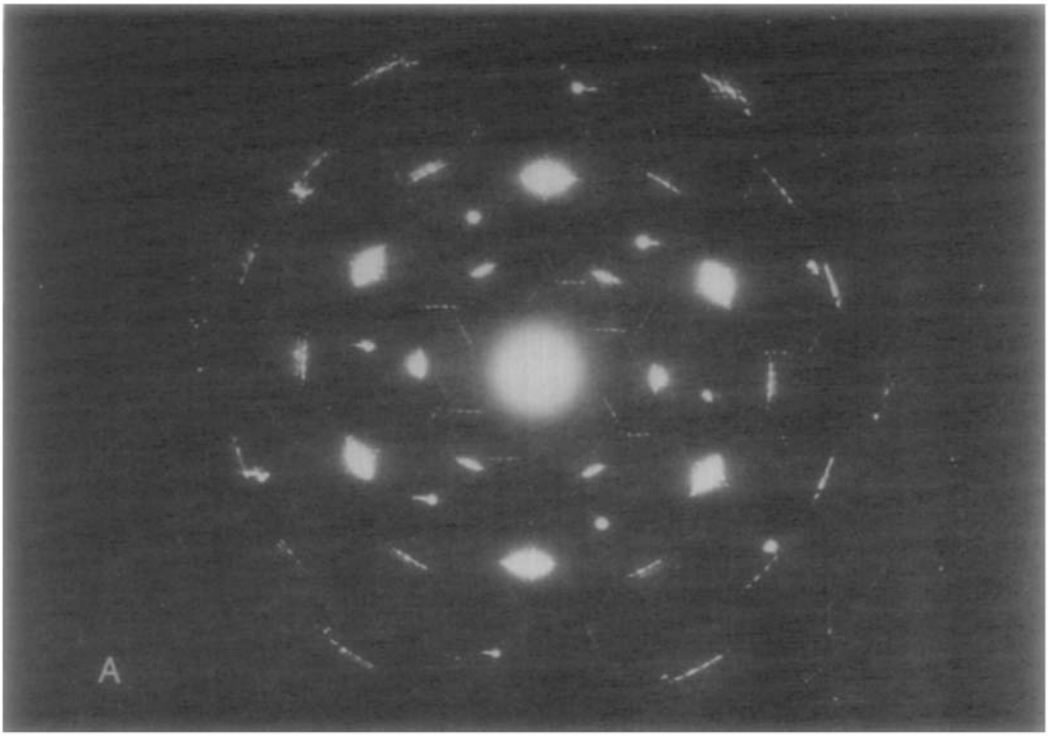

FIG. 4A. Complex, selected area electron diffraction pattern of graphite–ferric chloride intercalate produced by multiple diffraction effects and slight departure of the intercalating species from sixfold point symmetry.

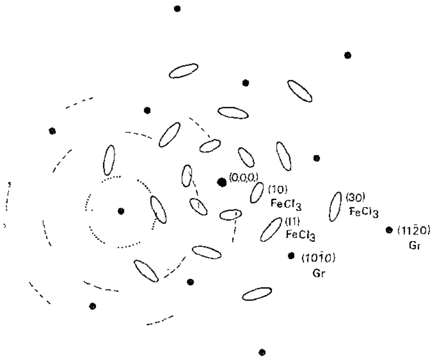

FIG. 4B. Schematic representation of multiple diffraction effects shown in Fig. 4A. Each graphite reflection (●) acts as a primary beam and produces further ferric chloride diffraction effects.

spacing of 0.52 nm. Figure 3C represents a possible configuration for these images.

Occasionally, extremely complex diffraction patterns were obtained (Fig. 4A) resulting from two additional factors namely, multiple diffraction and a slight departure of numerous ferric chloride layers from sixfold point symmetry. Each graphite reflection acts as a primary beam, producing around it further ferric chloride patterns identical with the one shown in Fig. 3A. This is illustrated schematically in Fig. 4B. The slight departure from sixfold symmetry leads to the appearance of Moire fringes with spacings of approximately 15 nm (Fig. 4C).

3.3 Graphite–Bromine

The structure of residual graphite–bromine has also been studied previously by electron diffraction (*5*) and identical results were obtained in our investigation. The diffraction pattern (Fig. 5) shows the usual graphite reflections together with intricate arrays of superlattice reflections and modulated streaks. Such effects indicate that bromine exists within the layers with a well-defined two dimensional structure which has a precise orientation relative to the adjacent graphite

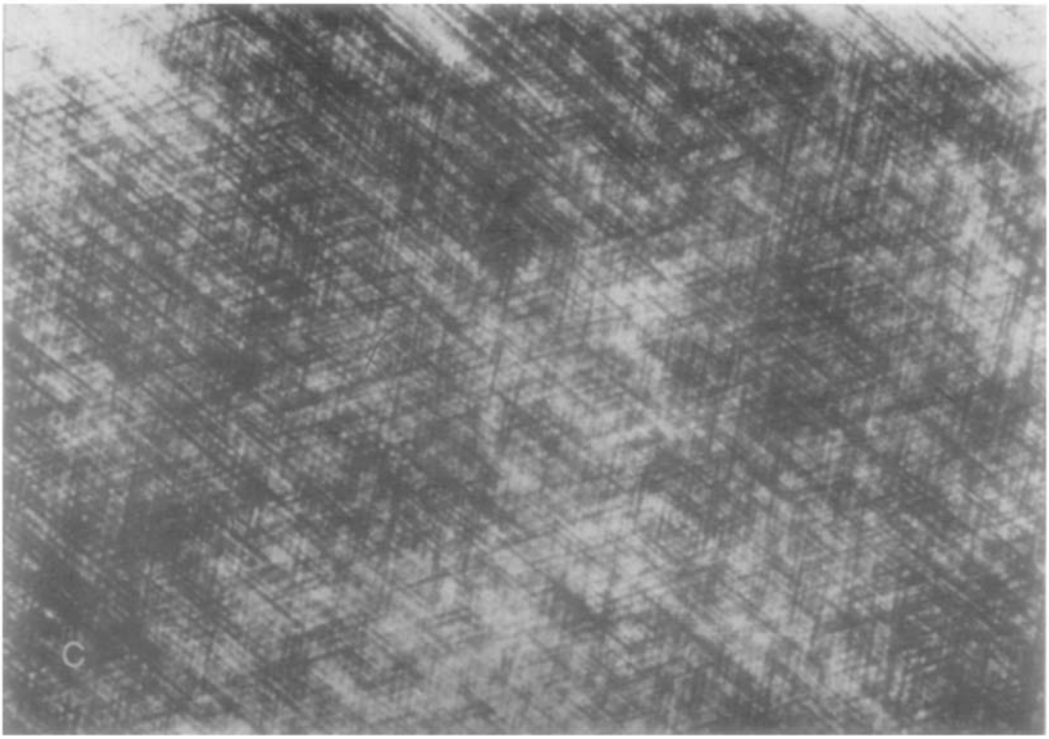

FIG. 4C. Moire fringes with spacings of approximately 15 nm caused by the departure of the ferric chloride intercalating species from sixfold point symmetry.

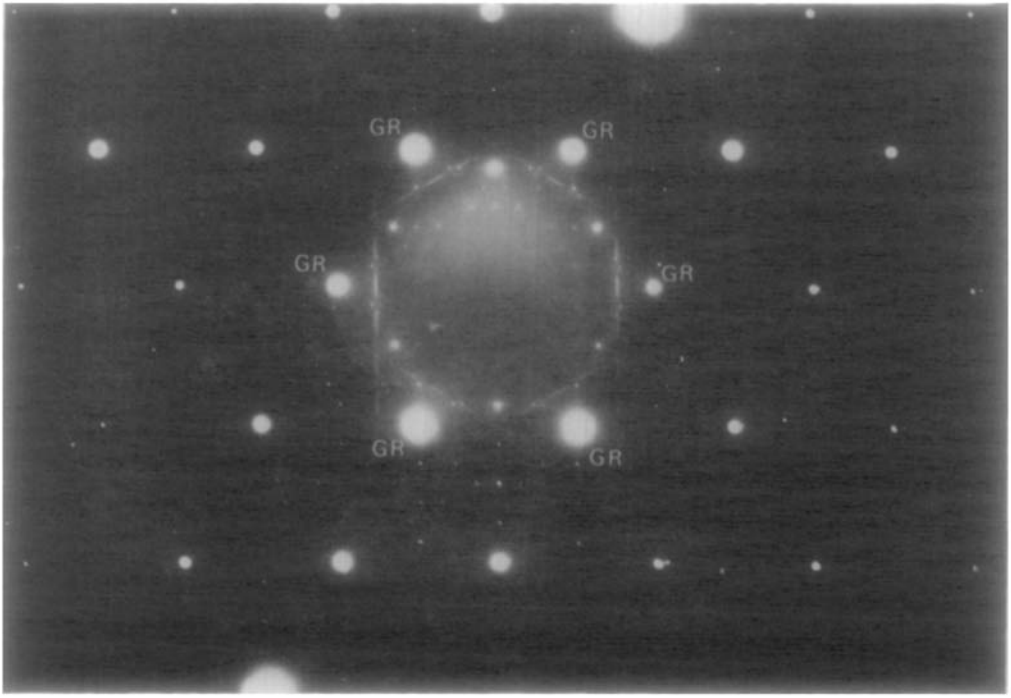

FIG. 5. Selected area electron diffraction pattern characteristic of graphite–bromine intercalate showing the usual graphite reflections together with intricate arrays of superlattice reflections.

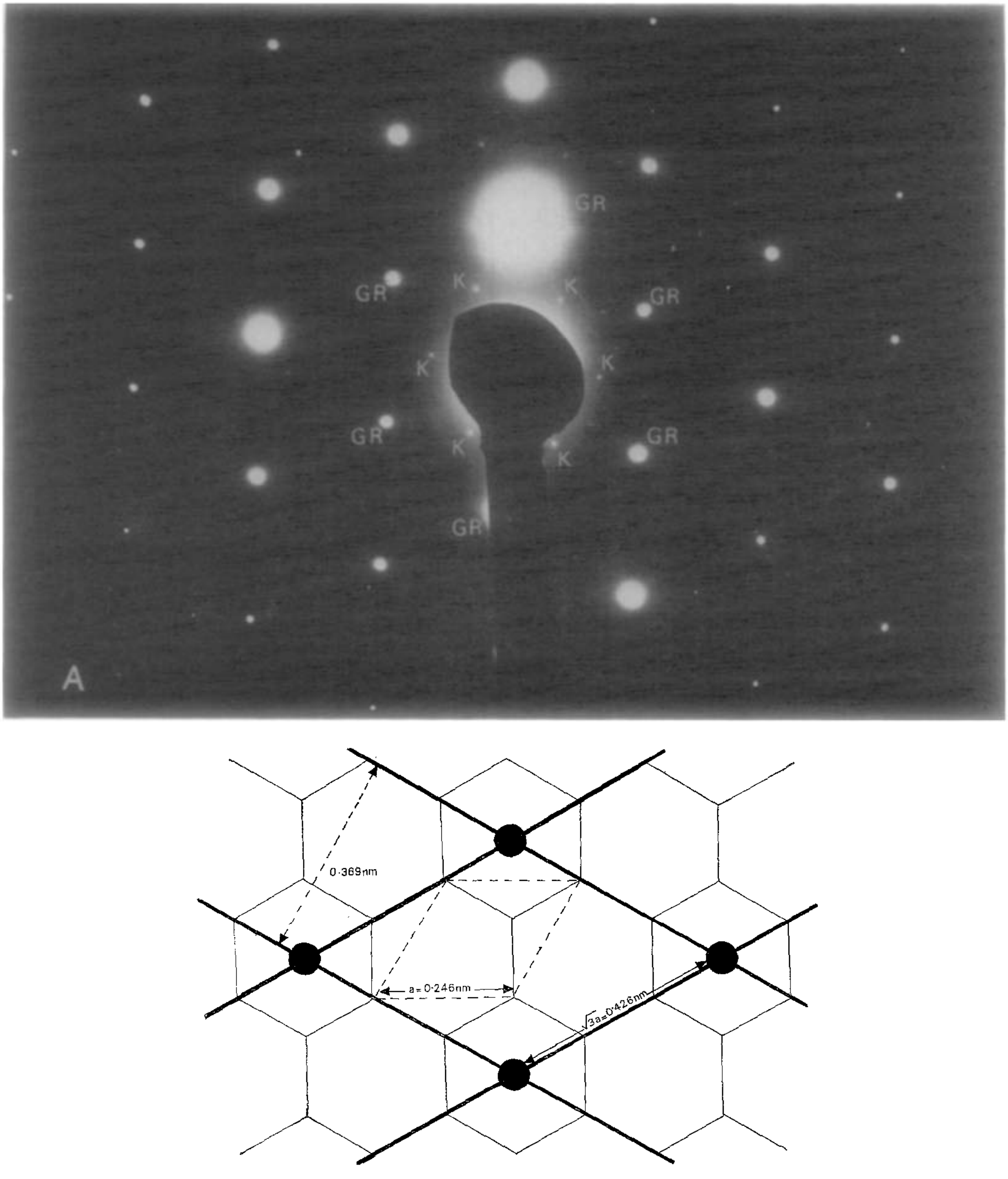

FIG. 6A. Selected area electron diffraction pattern of graphite–potassium intercalate showing that the potassium is ordered with a superlattice cell equal to $(3a)^{1/2}$ of graphite. B. Schematic representation of possible arrangement of potassium on the graphite lattice which would produce a $(3a)^{1/2}$ superlattice.

layers. The pattern is made up of three sets of reflections related to one another by rotation of 120° about the incident electron beam. Eeles and Turnbull (*5*) have interpreted the results in terms of a bromine chain structure and the modulated streaks observed in the diffraction pattern are due to the presence of random alterations of the chain directions between two possible configurations (See Fig. 11 of Ref. (*5*)).

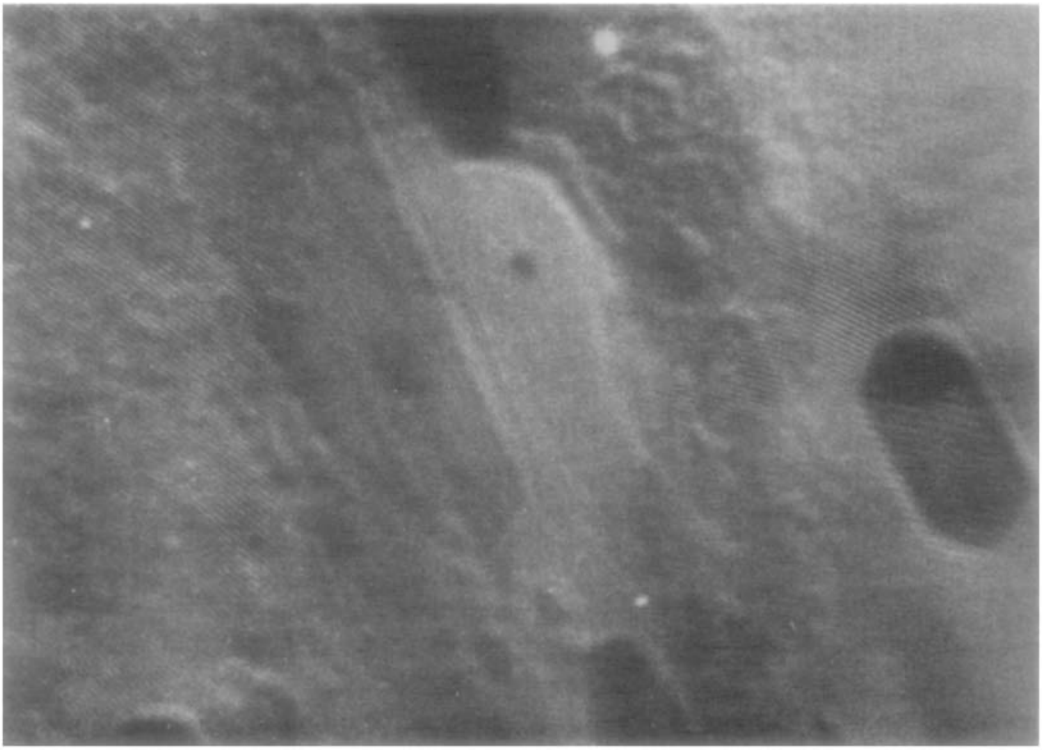

FIG. 7. Phase contrast high resolution image of graphite–potassium intercalate showing potassium contained in a hexagonal island and revealing the {10$\bar{1}$0} lattice planes of potassium with a spacing of 0.36 nm.

3.4. Graphite–potassium

Graphite–potassium is probably the most well-known graphite–metal intercalate. The electron diffraction pattern of this material (Fig. 6A) indicates that the potassium is ordered with respect to the graphite lattice and the potassium superlattice has a hexagonal unit cell with an *a* dimension equal to $(3a)^{1/2}$ of graphite, i.e., $a = 0.426$ nm. Potassium arranged on the graphite lattice as shown in Fig. 6B would produce such a superlattice. The potassium is occasionally contained in hexagonal islands with oriented edges which exhibit strong Moire effects (*4*). The {10$\bar{1}$0} lattice planes of potassium with a spacing of 0.36 nm is also revealed (Fig. 7) in neighbouring regions of the crystal but it is apparent that there are orientational differences between isolated potassium islands.

When graphite is saturated with potassium, each interlayer space contains the metal in an ordered arrangement but such a compound is unstable in vacuum and loses potassium readily to form the residue compound under discussion. A lattice image of the interlayer region of powdered graphite (SP1)–potassium (Fig. 8A) reveals that the intercalated potassium is located at random between the layers since some layer spacings are identical to the normal graphite value (0.34 nm), whereas other layer spaces contain intercalated potassium and the layers have swelled to accommodate the additional atoms. The corresponding diffraction pattern (Fig. 8B) shows streaking of the (000*l*) reflections indicative of this random intercalation.

3.5. Graphite–Potassium–Bromine

The possibility of forming an intercalate from more than one intercalating species had not been exploited until recently (*11*). When a graphite–bromine intercalate is treated with potassium we find that the diffraction pattern of the resulting intercalate

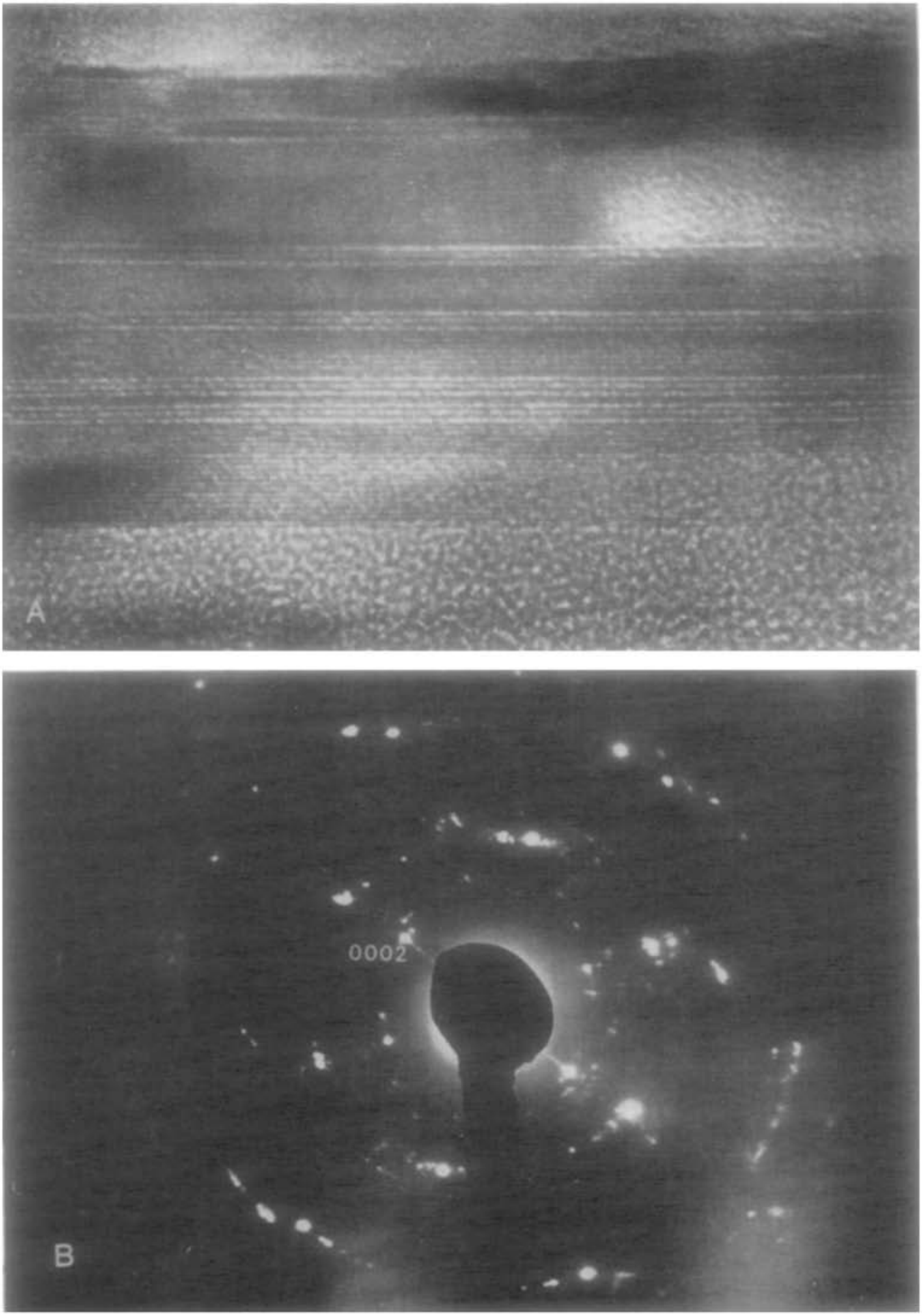

FIG. 8A. Phase contrast high-resolution lattice image of the interlayer region of graphite–potassium showing that the intercalated potassium is located at random between the layers. Regions containing potassium produce lighter layer images in the micrograph. B. Selected area electron diffraction pattern containing the area shown in Fig. 8A. Streaking of the (000*l*) reflections indicates random distribution of intercalating species.

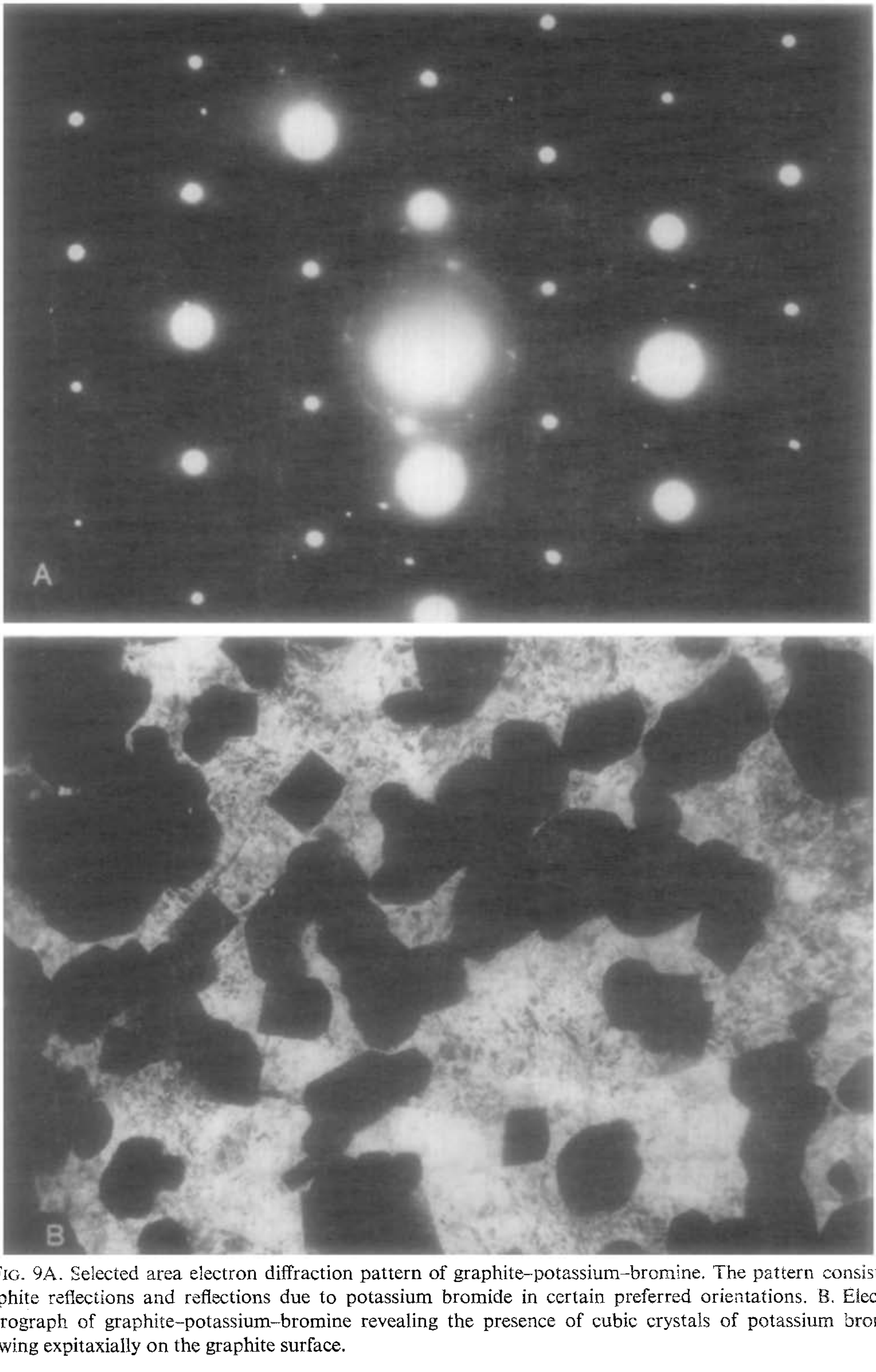

FIG. 9A. Selected area electron diffraction pattern of graphite–potassium–bromine. The pattern consists of graphite reflections and reflections due to potassium bromide in certain preferred orientations. B. Electron micrograph of graphite–potassium–bromine revealing the presence of cubic crystals of potassium bromide growing expitaxially on the graphite surface.

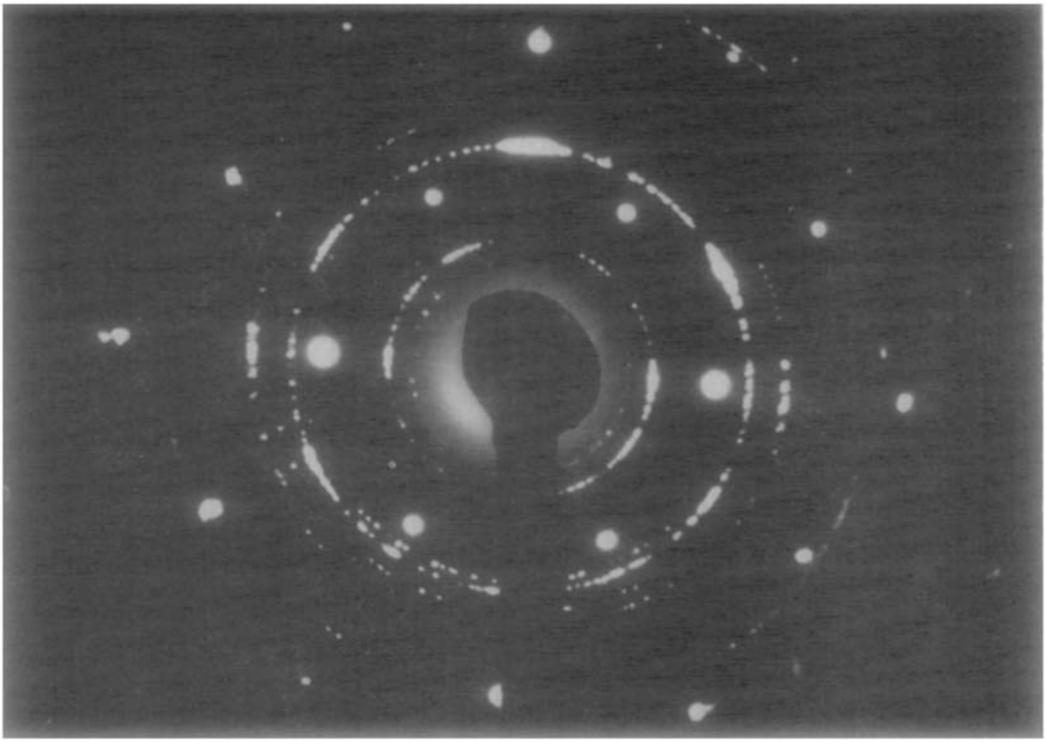

FIG. 10. Complex selected area electron diffraction pattern obtained from graphite–ferric chloride–potassium intercalate showing evidence for the presence of potassium chloride and free iron.

(Fig. 9A) consists of reflections arising from the graphite itself and other reflections from potassium bromide in certain preferred orientations. The electron micrographs obtained of this material, however, revealed the presence of cubic crystals of potassium bromide which had grown epitaxially on the graphite surface (Fig. 9B). It would appear that the resulting compound is not an intercalate and the potassium has extracted the bromine from the interlayer spaces to form potassium bromide on the surface.

3.6. Graphite–Ferric Chloride–Potassium

The ternary compound of potassium with graphite–ferric chloride has recently been used (*11*) as an effective catalyst for the synthesis of ammonia from hydrogen and nitrogen under less stringent conditions than those employed in the normal commercial process, but very little appears to be known about the microstructure of such a material. Even though its diffraction pattern is complicated (Fig. 10), it shows evidence for the presence of potassuim chloride and free iron. The presence of free iron has been confirmed by Mössbauer spectroscopy (*13*). We conclude, therefore, that potassium reduces ferric chloride to free iron and forms potassium chloride. The catalytic activity of this material is due, in all probability, to the presence of this free iron dispersed on the exterior surface of graphite thus affording a large and accessible iron surface for catalysis.

Acknowledgments

We thank the Science Research Council for its support, and Mr. J. LL. Jenkins for valuable technical assistance.

References

1. (a) R. C. CROFT, *Anst. J. Chem.* 9, 184 (1956); (b) G. R. HENNIG, *Prog. Inorg. Chem.* **1**, 125 (1959).

2. F. R. Gamble, J. H. Osiecki, and F. J. DiSalvo, *J. Chem. Phys.* **55**, 3525 (1971).

3. (a) A. Weiss, "Organic Geochemistry, Methods and Results" (G. Eglington and M. T. J. Murphy, Eds.), 734 Springer–Verlag, Berlin, 1969. (b) D. T. B. Tennakon, J. M. Thomas, M. J. Tricker, and J. O. Williams, *J. Chem. Soc.* (*Dalton*) 2207 (1974).

4. M. K. Halpin and G. M. Jenkins. Third Conf. Industrial Carbon and Graphite, p. 13, (*Soc. Chem. Ind*, *London*, 1970.

5. W. T. Eeles and J. A. Turnbull, *Proc. Roy. Soc.* **A283**, 179 (1965).

6. J. A. Turnbull and W. Y. Eeles; Second Conf. Industrial Carbon and Graphite, p. 173, Soc. Chem. Ind, London, 1966.

7. J. M. Cowley and J. A. Ibers, *Acta Cryst.* 421 (1956).

8. A. W. Syme Johnson, *Acta Cryst.* **23**, 770 (1967).

9. J. G. Hooley, "Chemistry and Physics of Carbon" (P. L. Walker, Jr., Ed.), Vol. 5, p. 321, Dekker, New York, 1969.

10. M. Heerschap and P. Delavignette, *Carbon* **5**, 383 (1967).

11. M. Ichikawa, T. Kondo, and K. Kawaso, *J.C.S. Chem. Commun.* 176 (1972).

12. J. M. Thomas, "Chemistry and Physics of Carbon" (P. L. Walker, Jr., Ed.), Vol. 1, p. 121, Dekker, New York, 1965.

13. M. J. Tricker, E. L. Evans, P. Cadman, N. C. Davies, and B. Bach, *Carbon* **12**, 499 (1974).